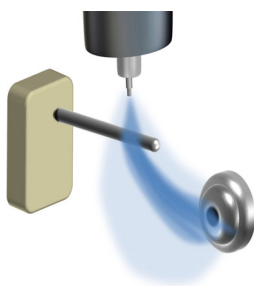


RESEARCH ARTICLE

Atmospheric Pressure Ionization Using a High Voltage Target Compared to Electrospray Ionization

Arnaud Lubin,¹ Steve Bajic,² Deirdre Cabooter,³ Patrick Augustijns,³ Filip Cuyckens¹¹Discovery Sciences, Janssen Research and Development, Turnhoutseweg 30, B-2340, Beerse, Belgium²Waters Corporation, Wilmslow, UK³Department of Pharmaceutical and Pharmacological Sciences, KU Leuven, Leuven, Belgium

Abstract. A new atmospheric pressure ionization (API) source, viz. UniSpray, was evaluated for mass spectrometry (MS) analysis of pharmaceutical compounds by head-to-head comparison with electrospray ionization (ESI) on the same high-resolution MS system. The atmospheric pressure ionization source is composed of a grounded nebulizer spraying onto a high voltage, cylindrical stainless steel target. Molecules are ionized in a similar fashion to electrospray ionization, predominantly producing protonated or deprotonated species. Adduct formation (e.g., proton and sodium adducts) and in-source fragmentation is shown to be almost identical between the two sources. The performance of the new API source was compared with electrospray by infusion of a mix of 22 pharmaceutical compounds with a wide variety of functional groups and physico-chemical properties (molecular weight, logP, and pKa) in more than 100 different conditions (mobile phase strength, solvents, pH, and flow rate). The new API source shows an intensity gain of a factor 2.2 compared with ESI considering all conditions on all compounds tested. Finally, some hypotheses on the ionization mechanism, similarities, and differences with ESI, are discussed.

Keywords: UniSpray, Electrospray, ESI, Mass spectrometry, Ionization, Source, MS, API

Received: 2 June 2016/Revised: 17 October 2016/Accepted: 18 October 2016/Published Online: 28 November 2016

Introduction

Despite a prominent use in today's liquid chromatography-mass spectrometry (LC-MS) instruments, electrospray ionization (ESI) interfaces suffer from low ionization and transmission efficiency [1–4]. A lot of efforts have been driven to improve transmission efficiency by sampling and transporting ions from atmospheric pressure into the vacuum chamber more effectively [5–10]. To address the poor efficiency of electrospray, nanospray was developed as it was observed that the formation of smaller droplets at low flow rates largely increases the ionization efficiency [11, 12]. However, nanospray is not ideal for high throughput analysis since low flow rates in combination with system dead volume, intrinsically present in any system, result in (much) longer run times,

and also user friendliness and robustness are affected going to smaller internal tubing and columns diameter. Therefore, it remains mainly limited to applications where only very small samples are available, such as the analysis of proteins.

The electrospray ionization source design was constantly improved in order to increase ionization efficiency, which involves mainly modification of the sprayer orientation as well as position and number of heated gas inlets. Excellent reviews on the development of electrospray ionization and other atmospheric pressure ionization (API) sources are available [4, 13–16].

Recently, an atmospheric pressure ionization source using a high voltage target has been introduced [17–19]. The newly developed source, recently commercialized as UniSpray, is composed of a grounded nebulizer spraying onto a high voltage target and has an ionization mechanism similar to ESI but promotes droplet break-up and desolvation via additional Coandă and vortex effects [20]. A similar approach has also been developed using sonic spray ionization (SSI) and a modified atmospheric solid analysis probe (ASAP) for the analysis of proteins and peptides [21]. The profile of the mass spectra was similar to that obtained with SSI but matched the signal

Electronic supplementary material The online version of this article (doi:10.1007/s13361-016-1537-3) contains supplementary material, which is available to authorized users.

Correspondence to: Filip Cuyckens; e-mail: FCUYCKEN@its.jnj.com

intensity of ESI, which was 100 times higher than SSI without obstruction.

The aim of this paper is to introduce in detail a new API source, which has previously shown a significant gain in signal intensity when directly compared with ESI on a limited set of analytes [19]. The design of the new API source is presented thoroughly with description of the general behavior (ion formation and in-source fragmentation) and required tuning. The performance of the new API source was compared with electrospray ionization by infusions of a mix of pharmaceutical compounds with a wide variety of functional groups and physico-chemical properties (molecular weight, logP, and pKa) in different conditions (mobile phase strength, solvents, pH, and flow rate) with the objective to find correlations between chemical structure and the relative sensitivity of both sources for different solvent conditions. Finally, some hypotheses on the ionization mechanism, similarities, and differences with ESI, are discussed.

Experimental

Chemicals and Reagents

Acetonitrile (ACN), formic acid (FA), and methanol (MeOH), all of analytical grade, were purchased from Merck (Darmstadt, Germany). Ammonium acetate, also of analytical grade, was purchased from VWR (Leuven, Belgium). Amitriptyline hydrochloride, atenolol, buspirone hydrochloride, cyclosporine A, diclofenac sodium salt, haloperidol, ketoconazole, loperamide hydrochloride, progesterone, propranolol hydrochloride, and tolbutamide were synthesized internally at Janssen Pharmaceutica (Beerse, Belgium). Fluoxetine hydrochloride and lincomycin hydrochloride, acetaminophen, amiodarone hydrochloride, enalapril, norfloxacin, quinidine, terfenadine, and trazodone hydrochloride were obtained from Sigma (Steinheim, Germany), and warfarin from DuPont Pharma (Wilmington, DE, USA). Ultrapure water (H₂O) was produced with a MilliQ system (Millipore, Billerica, MA, USA).

Instrumentation

All experiments were performed on a Synapt-G2 quadrupole time-of-flight mass spectrometer equipped with an ESI source or a UniSpray source (all Waters, Milford, MA, USA). The mass spectrometer was operated in both negative and positive full-scan mode using HR-MS detection in sensitivity mode (resolution approximately 10,000 at m/z 556). All peak heights were extracted manually from average full-scan MS spectra obtained from the last 30 s of every 5% step gradient window. Data processing was done in Unifi 1.8 (Waters, Milford, MA, USA).

An Acquity UPLC system (Waters, Milford, MA, USA) and a syringe pump (Harvard Apparatus Pump 11 Elite, MA, USA) equipped with a 500 μ L glass syringe (Hamilton, NV, USA) were used for the infusions.

UniSpray Source Design

The new atmospheric pressure ionization source used in this study is shown schematically in Figure 1 [20]. A high velocity nebulized jet from a grounded sprayer asymmetrically impacts a cylindrical metal target that is held at a high voltage and is located between the sprayer and the ion inlet orifice of the mass spectrometer. Although the schematic of Figure 1 shows a glancing impact, it should be noted that in practice, the majority of the spray column will impact the upper right hand quadrant of the target.

The pneumatically assisted nebulizer is formed from a 130 μ m i.d. by 220 μ m o.d. liquid delivery capillary (stainless steel) that is surrounded by a 330 μ m i.d. nebulizer tube (stainless steel) with a restriction length of 10 mm. Nitrogen gas is delivered to the nebulizer tube at a gauge pressure of 7 bars. Under these conditions, the nebulizer gas velocity will be near-supersonic for sprayer/target distances of 1–3 mm (Figure 1). The nebulizer is surrounded by an annular heater that delivers hot nitrogen gas at a flow rate of typically 1200 L.h⁻¹.

The 1.6 mm-diameter, 35 mm-long, cylindrical high voltage (HV) target is constructed from a cold-drawn, 316 L stainless steel wire that is polished to a near-mirror finish with 1 μ m-grade lapping paper. The target is connected to a 0–5 kV DC power supply via a 47 M Ω current-limiting resistor. Since the target has a low thermal conductance to the source housing, it rapidly reaches an equilibrium temperature that is equal to the local temperature of the heater gas (typically >250 °C for a set heater temperature of 500 °C). Ions and charged droplets formed upon impact are directed towards the ion inlet, which is surrounded by a cone gas nozzle that supports a nitrogen drying gas flow of 150 L.h⁻¹.

Infusion Experiments

The following setup (see Supplementary Figure 1) was used for all the experiments: a UPLC pump and a syringe pump were connected via a PEEK T-connector to deliver a constant flow to the mass spectrometer. The syringe pump was used to deliver a mixture of compounds at a flow rate of 5 μ L.min⁻¹ in all experiments. The UPLC pump was used to obtain the different gradient and solvent conditions at a total flow rate of 100, 400, or 800 μ L.min⁻¹. For each flow rate, a gradient from 5% to 95% of organic phase in steps of 5% was run with the following solvent combinations: H₂O/MeOH or H₂O/ACN. Three pHs were tested with a constant concentration over the gradient of either 0.1% of formic acid (pH = 2.85) or 10 mM of ammonium acetate (pH = 7 or pH = 9) adjusted with ammonia. Thus, a total of 18 experiments were performed per ionization mode (positive and negative).

Small molecule pharmaceutical compounds with a wide range of physico-chemical properties (molecular weight, logP, pKa, and functional groups) were chosen to prepare two mixes (see Table 1): one mix of 16 compounds for the positive ion mode and one containing 7 compounds for evaluation of the negative ion mode. Both mixes were prepared at three different concentration levels in order to give the same

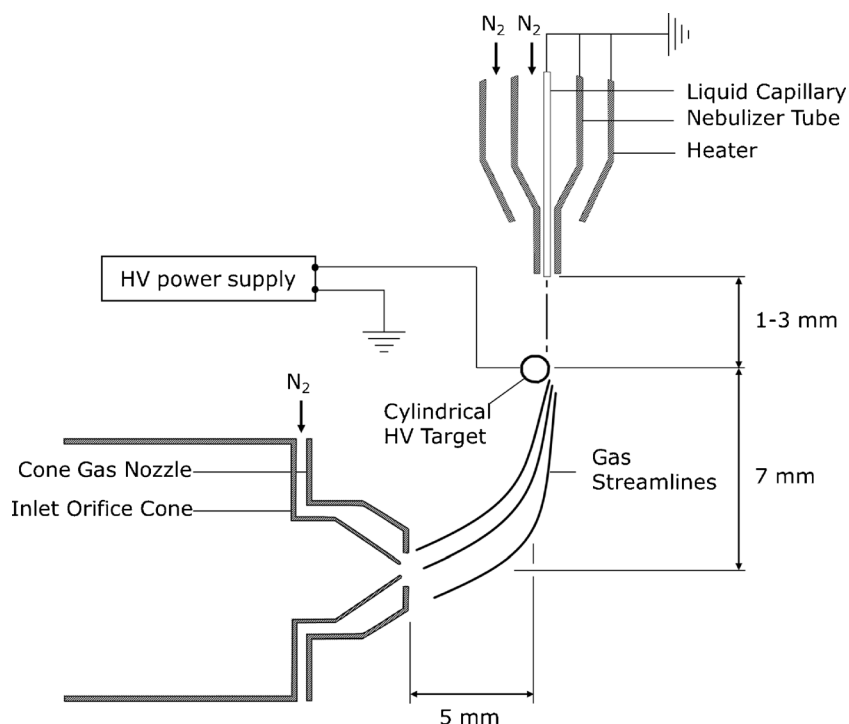


Figure 1. Schematic representation of the UniSpray source

final concentration at the three different flow rates (100, 400, or 800 $\mu\text{L}\cdot\text{min}^{-1}$) tested. The mixes prepared for the infusions at 800 $\mu\text{L}\cdot\text{min}^{-1}$ were diluted for the experiments at 400 $\mu\text{L}\cdot\text{min}^{-1}$ and 100 $\mu\text{L}\cdot\text{min}^{-1}$ in order to obtain a signal well within the linear range of the mass spectrometer (i.e., good signal-to-noise ratios in all conditions without detector saturation).

Table 1. List of Compounds Used for the Infusion Experiments with Their Exact Mass, logP, pKa, and the Concentration Infused in the Mass Spectrometer. LogP and pKa Experimental Values are Extracted from the Literature

Compound	Exact mass	LogP _{exp}	pKa _{exp}	Concentration (ng/mL)
Amiodarone	645.0237	7.80	8.7	78
Amitriptyline	277.1830	4.92	9.4	30
Atenolol	266.1630	0.16	9.6	90
Buspirone	385.2478	2.63	1.9/7.6	40
Cyclosporine A	1201.8414	2.92	-	330
Fluoxetine	309.1340	4.50	9.6	290
Haloperidol	375.1401	3.36	8.3	100
Ketoconazole	530.1488	3.73	2.9/6.5	250
Lincomycin (pos)	406.2138	0.20	7.7	70
Loperamide	476.2231	3.90	8.9	10
Norfloxacin	319.1332	1.49	6.1/8.3	110
Progesterone	314.2246	3.97	-	140
Propranolol	259.1572	3.20	9.6	70
Quinidine	324.1838	2.88	4.2/8.3	50
Terfenadine	471.3137	5.52	8.6	30
Trazodone	371.1513	1.66	6.8	90
Acetaminophen	151.0633	0.51	9.4	2270
Atenolol	266.1630	0.16	9.6	1819
Diclofenac	295.0167	4.2	4	960
Lincomycin (neg)	406.2138	0.2	7.7	2500
Tolbutamide	270.1038	2.34	5.4	170
Warfarin	308.1049	2.7	4.9	150
Enalapril	376.1998	0.27	3.1/5.5	1250

Tuning of the UniSpray and ESI source was done at each experimental flow rate for the mix of compounds analyzed, using the same solvent composition as intended for the experiment to be performed. At every flow rate, both sources were tuned to achieve optimal signal intensity for the mix by adjusting source temperature, gas flows, gas temperature, extraction cone, sampling cone, position of the spray, protrusion of the capillary and capillary voltage (see Supplementary Table 1).

All experiments were performed back-to-back on both sources; one flow rate per ionization mode (+ or -) per day (total of 6 d). The first experiment of each day was partially reproduced at the end of the day to ensure that variation of the absolute intensity was less than or equal to 10% over the day. The intensity of the calibration mixture of the instrument (sodium formate) was checked every day to guarantee there was no loss in MS detector sensitivity between days.

Results and Discussion

Tuning of the UniSpray Source

In order to optimize source sensitivity, the most important tuning parameter to adjust is the point at which the collimated spray impacts on the cylindrical target. The maximum signal intensity is typically obtained when the spray is asymmetrically positioned such that it impacts on the upper right quadrant of the target (see Supplementary Figure 2). Under these conditions, the gas flow becomes attached to a portion of the curved surface and results in asymmetric gas streamlines in the wake

that are directed towards the ion inlet orifice. This flow phenomenon is known as the Coandă effect [22, 23].

The voltage applied on the rod was found to be less critical than the capillary voltage on the ESI source. When tuning from 0.5 to 2 kV, the optimal voltage for all experiments performed with the new API source was 1 kV (see Supplementary Table 1). Similar to ESI, the protrusion of the capillary has a clear impact on signal intensity and should be adjusted accordingly upon installation. With the UniSpray source, the best spray is generally obtained when the capillary is barely protruding from the nebulizer tube. Other source parameters such as source temperature, gas flows, gas temperature, extraction cone, and sampling cone voltage were at nearly identical values on both sources.

Tuning with both sources is very similar; only one more dimension on the spray axis has to be tuned with the new API source, whereas other parameters were less critical than with ESI. Finally, when tuning the spray axis, no significant compound dependence on the signal was observed.

UniSpray Behavior

Even though the source has previously shown radical ion formation for compounds traditionally analyzed by APCI or APPI (e.g., benzo(ghi)perylene, 2-fluorophenylboronic acid, 2-chlorophenylboronic acid...) [17], the mix of compounds used in this study ionized identically on both UniSpray and ESI sources. The same adducts such as $[M + H]^+$, $[M + Na]^+$, or $[M + K]^+$ were observed in similar ratios on the two sources. Compounds known to undergo in-source fragmentation such as tolbutamide or diclofenac showed the same fragments at similar relative intensities on both sources (see Supplementary Figure 3).

UniSpray-ESI Comparison

Each of the 36 experiments performed has generated at least 19 data points per compound, which represents more than 17,700 MS peaks processed. In order to compare both sources, data have been compiled in graphs to show the differences and trends observed. Classic non-Tukey's box plots are used to represent the distribution of the data points [24, 25]. It is important to note that signal intensity gain scales are used in Figures 2 and 3 as the "y" axis. A relative difference scale in percentage is used to show the absolute gain or loss of the new API source signal in comparison to ESI; for example a 100% "y" value correlates with MS peaks twice more intense with the new API source than with ESI. Following the same logic, -200% is associated with an ESI signal three times more intense than the signal observed on the new API source, whereas 0% means that the same peak intensity is observed on both sources. This scale is chosen over a ratio or log scale because the ponderation of the data points will not mislead the reader, especially when ESI signal is more intense.

Figure 2 shows pooled data for the intensity gain per compound for all conditions (flow rates and solvents used). All the

compounds, except progesterone and lincomycin, give overall a higher signal with the new API source.

In Figure 3, the intensity gain is plotted against the different solvent compositions for all compounds and flow rates (pooled data) for data averaged along the gradient. In these graphs, except for ACN/H₂O with formic acid in negative ionization mode, a net gain in signal intensity is observable for the UniSpray source. The distribution of the data points indicates higher gain at higher pH for both H₂O/ACN and H₂O/MeOH solvents for a gain of 137% in positive mode and 95% in negative mode with an average around 116% gain (corresponding to a factor 2.2). The box plots, which represent around 1700 points each, show that the data are mostly condensed over a 100%–150% gain range. The extreme values are obtained in conditions when ionization is not optimal, such as high aqueous percentages.

The last graphs (Figure 4) display the intensity peak ratios between UniSpray and ESI ($I_{\text{UniSpray}}/I_{\text{ESI}}$) for an average of all compounds and solvents along the gradient. From these graphs it can be concluded that the signal intensity observed with the new API source is on average higher than the ESI signal all over the different gradients tested with relatively higher gains in aqueous conditions. It is of noticeable importance to point out that a minimum flow rate is needed to visually observe a proper impact of the spray on the HV target with the new API source.

As seen for data obtained at a flow rate of 100 $\mu\text{L}\cdot\text{min}^{-1}$ in negative mode, the ratio ($I_{\text{UniSpray}}/I_{\text{ESI}}$) in Figure 4 exhibits a characteristic that is not consistent with the data collected at the two higher flow rates.

In summary, the compounds studied show a signal intensity gain (Figure 2) in favor of the new API source. Even though an average of around 116% gain corresponding to a factor 2.2 is observed, compounds individually show different gains depending on the conditions. No correlation could be found between the different gains (ESI or UniSpray) observed and the molecular weight, functional groups, pKa, or logP of the studied compounds. This implies that complex ionization mechanisms are involved with the UniSpray source. Some tentative hypotheses on the ionization mechanism of the new API source are given below.

UniSpray Ionization Mechanism

Since the qualitative characteristics of the mass spectra were the same for both source types used in this study, it would be reasonable to assume that the new API source can enhance the ionization processes already existing in high flow rate ESI sources. In the traditional ESI model, charged droplets are formed by charge separation in the high electric field region at the tip of the liquid capillary. At very low flow rates ($<1 \mu\text{L}\cdot\text{min}^{-1}$), this process proceeds with extremely high efficiency to yield highly-charged, sub-micron droplets that almost instantaneously give rise to gas-phase ions due to Rayleigh disintegration processes [26]. However, at the high flow rates used in this study (100–800 $\mu\text{L}\cdot\text{min}^{-1}$), it is

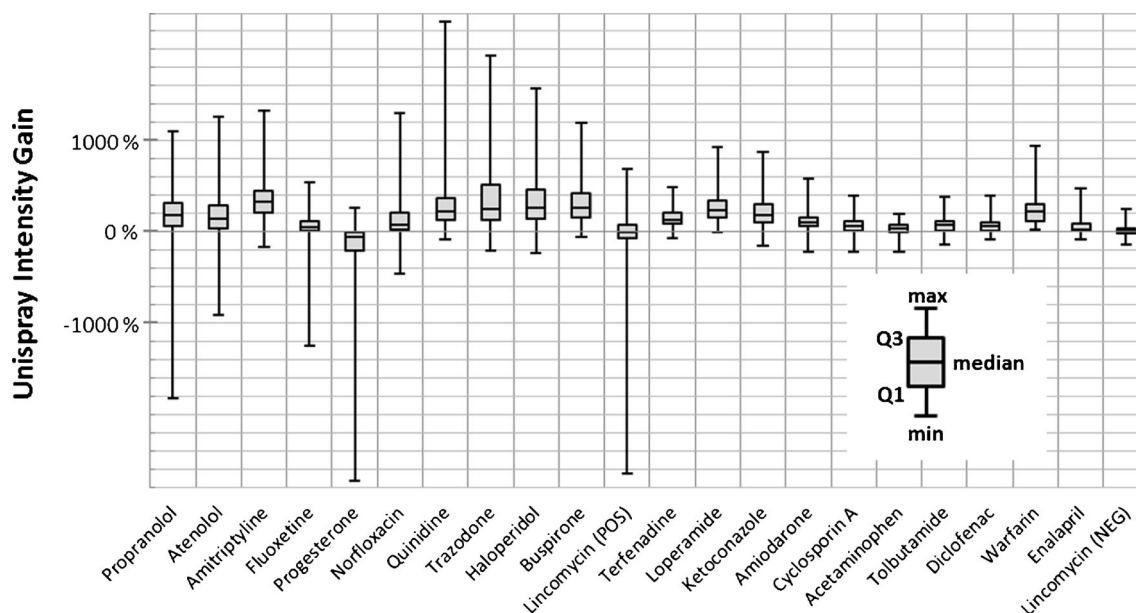


Figure 2. UniSpray intensity gain expressed in relative intensity, all conditions pooled per compound. Non-Tukey's box plots are used to better visualize the repartition of the data points

necessary to use a high velocity nebulizer gas flow to atomize the liquid flow, a process which is known to produce larger droplets with lower charges per unit volume and, hence, lower ionization efficiency [27].

Whilst the use of a high velocity gas flow is advantageous from an atomization viewpoint, it has the disadvantage of reducing the residence time of droplets between the ESI capillary and the ion inlet orifice of the mass spectrometer, which, in turn, reduces the time available for droplet evaporation that is critical for the Rayleigh disintegration process. In-house measurements, using phase Doppler anemometry (PDA) and laser diffraction particle sizing (LDPS) have revealed that the ESI and UniSpray nebulizers typically produce initial droplet size distributions that peak at typical diameters of $d_0 = 10 \mu\text{m}$ in the volume domain and $d_0 = 1 \mu\text{m}$ in the number domain. Furthermore, these measurements reveal that droplets on the

spray axis can have average velocities in excess of $100 \text{ m}\cdot\text{s}^{-1}$, which corresponds to a residence time of $<100 \mu\text{s}$ for the sources used in this study (ignoring any recirculation effects). Using evaporation models available in the literature [28], it can be shown that water droplets with initial diameters of 10 and $0.4 \mu\text{m}$ will evaporate to diameters of 9.99 and $0.19 \mu\text{m}$, respectively, after a $100 \mu\text{s}$ residence time. In essence, this would suggest that a $100 \mu\text{s}$ residence time is totally inadequate for efficient evaporation of the larger droplets in the ESI spray. Whilst this laminar-flow evaporation model may be oversimplified, it would suggest that only sub-micron droplets would participate in the production of gas-phase ions by the ESI process. Since the sub-micron population accounts for typically $<1\%$ of the total sprayed volume, this would contribute to the low ionization efficiency typically observed with high flow rate ESI compared with nanospray ESI

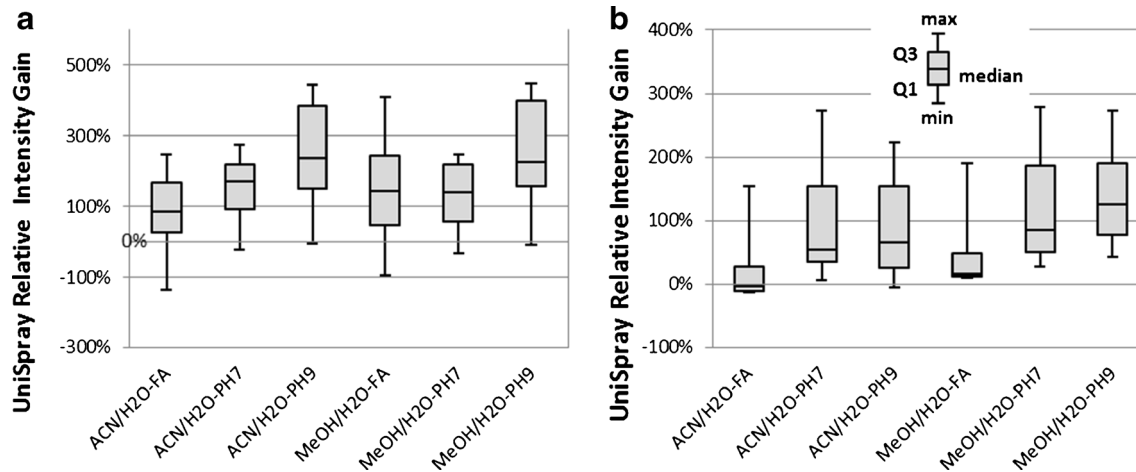


Figure 3. UniSpray intensity gain expressed in relative intensity, all conditions pooled per solvent for (a) positive and (b) negative ion modes. Non-Tukey's box plots are used to better visualize the repartition of the data points

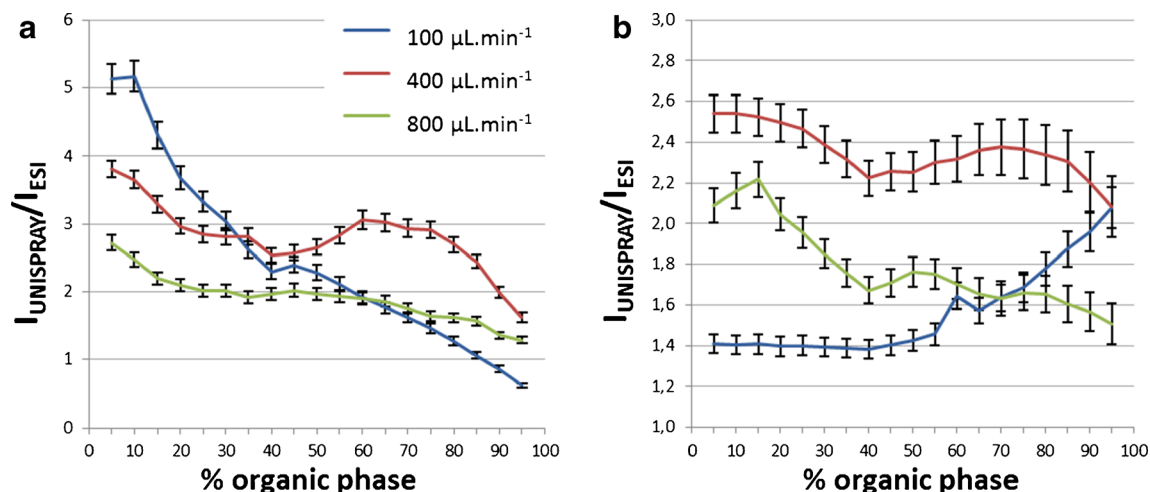


Figure 4. Average intensity ratio with standard error of UniSpray over ESI plotted versus the percentage of organic phase for (a) positive and (b) negative ion modes

(<1 $\mu\text{L}\cdot\text{min}^{-1}$) where submicron-sized droplets contribute significantly to the volume distribution.

The above inefficiency argument was the original inspiration for the UniSpray ionization source that compels high velocity droplets to impact onto a hot metallic surface, which results in their break-up into smaller secondary droplets that can be evaporated more efficiently at low residence times. A number of groups have studied the break-up of water droplets on heated stainless steel surfaces [29]. They experimentally determined that the number of visible secondary droplets (N_{vis}) produced per impact was directly proportional to the droplet Weber number, which is directly proportional to the droplet diameter and the square of its velocity. In our case, a water droplet with a diameter of 4 μm and a velocity of 100 $\text{m}\cdot\text{s}^{-1}$ would have a Weber number of 571 and would give rise to 35 visible secondary droplets on impact with the hot target. If we consider a simple linear break-up model, this would result in secondary droplets with diameters of the order 1.2 μm . More realistically, a skewed Gaussian distribution for the secondary population would contain submicron droplets in addition to invisible droplets that could not be detected by the experimental method used in the above work.

Although the impact of high Weber number droplets is believed to be a critical feature of the enhanced sensitivity observed with the UniSpray source, it should be noted that early in-house experiments with flat-plate stainless steel targets did not give rise to significant signal enhancements over ESI. In this respect, it is believed that the geometrical form of the UniSpray source, shown schematically in Figure 1, plays a significant part in the enhanced performance of the source. In particular, it is believed that the curved profile of the target and the off-axis, perpendicular cross-flow arrangement between the sprayer and the target give rise to two important gas flow phenomena that may aid the break-up and desolvation of liquid droplets in the source, viz. the Coandă effect [30] and surface microvortices [31].

As a water droplet evaporates, the gas surrounding the droplet can rapidly become saturated with water vapor, which

ultimately reduces the rate of evaporation due to recondensation on the droplet surface. In API sources, this effect is minimized by supplying a flow of heated dry nitrogen gas to the nebulized spray where the nitrogen becomes “entrained” into the nebulizer flow because of the low pressure created by the high velocity nebulizing jet. In the case of Coandă flow attachment to a curved surface, as occurs at the UniSpray HV target, it is the imbalance of the entrainment flow where flow cannot penetrate from one side that ultimately leads to a deflection of the gas streamlines towards the target surface. This effect is known to create a stronger total entrainment flow compared with a free jet, which could aid the droplet desolvation process by enhanced mixing with the water vapor. The Coandă effect at the curved target could also improve source sensitivity by (1) enhanced mixing in the turbulent wake (vortex shedding) that is observed at the high Reynolds numbers associated with the near-supersonic gas velocity, and (2) the “beam steering” effect that directs ions and charged droplets towards the ion inlet orifice. It is important to note that the vortex shedding in the gas flow wake is a different phenomenon to the surface microvortices that will be described below.

For a cylinder in cross-flow, a uniform gas flow will become inherently unstable (three-dimensional) in the stagnation region where the flow becomes attached to the curved surface. These instabilities take the form of a series of counter-rotating vortices, the axes of rotation of which are aligned with the streamlines of the gas flow [32]. The disturbance wavelength, λ , between adjacent counter-rotating pairs is known to be inversely proportional to the square root of the local Reynolds number [31]. For near-supersonic gas velocities and a target diameter of 1.6 mm, it can be estimated that the surface vortices on the UniSpray target will be microvortices with an approximate scale of $\lambda = 37 \mu\text{m}$. First, this disturbance dimension is significant in that it is of the same order as the size of the initial or secondary droplets and thus may impart energy into the droplets to aid break-up. Second, droplets that enter this stagnation flow region will travel at a lower velocity than those that

remain in the free flow and will be subjected to enhanced heat transfer from the hot target surface and further mixing with the entrained nitrogen gas as described above.

In this section, we have sought to provide an explanation of how the unique geometry of the UniSpray source gives rise to a number of hydrodynamic and aerodynamic phenomena that may aid in the nebulization and desolvation of primary droplets from the liquid capillary. Whilst these hypotheses may be supported by the observation of a greater increase in sensitivity over ESI for high aqueous mobile phases where nebulization and desolvation are particularly difficult, it is clear that the understanding of the experimental data is far from complete. The processes described thus far are highly interdependent and highly complex from a modeling perspective. In particular, the exact role of the metallic surface in the flow stagnation region is not fully understood. It is known that any significant damage (gouging) to the target surface in the stagnation region, which subtends an arc of approximately 45° from the spray impact point to the point of flow detachment, will severely affect the source performance. While some droplet charging originates at the point of nebulization, other processes that resemble electrospray, spray electrification [33], statistical charging as observed in sonic spray [34] or thermospray ionization [35], may account for droplet charging at the point of impact on the high voltage target. Work will continue with a view to gaining a thorough understanding of these ionization processes.

Conclusion

On average, a higher signal intensity was observed on the new API source that will lead to better sensitivity if selectivity is warranted. The latter depends on the type of mass spectrometer used (e.g., high resolution MS, MSⁿ, ion mobility capabilities, etc.) and the nature of the sample (background). Therefore, signal intensities were reported, giving an honest back to back comparison with ESI independent of any parameters that are not related to the source.

Research on the droplet break-up mechanism is mainly focusing on the applications of inkjet printing and other aerosol techniques, aeronautic and fuel injectors [36, 37]. More research on high velocity micro-droplets would be valued to better understand the ionization mechanism of UniSpray and similar sources. Meanwhile, similar work on different classes of compounds (e.g., peptides and proteins), can highlight potential applications and give additional information on the ionization mechanism of the new API source.

Acknowledgments

The authors acknowledge the help and support of Ed Sprake and Marijn Van Hulle (Waters) in getting the hardware installed and operational. The authors also acknowledge ARIADME, a European FP7 ITN Community's Seventh Framework Program financed under grant No. 607517.

References

- Page, J.S., Kelly, R.T., Tang, K., Smith, R.D.: Ionization and transmission efficiency in an electrospray ionization–mass spectrometry interface. *J. Am. Soc. Mass Spectrom.* **18**(9), 1582–1590 (2007)
- Oss, M., Krueve, A., Herodes, K., Leito, I.: Electrospray ionization efficiency scale of organic compounds. *Anal. Chem.* **82**(7), 2865–2872 (2010)
- Leito, I., Herodes, K., Huopola, M., Virro, K., Kunnas, A., Krueve, A., Tanner, R.: Towards the electrospray ionization mass spectrometry ionization efficiency scale of organic compounds. *Rapid Commun. Mass Spectrom.* **22**, 379–384 (2008)
- Covey, T.R., Thomson, B.A., Schneider, B.B.: Atmospheric pressure ion sources. *Mass Spectrom. Rev.* **28**(6), 870–897 (2009)
- Campargue, R.: Progress in over-expanded supersonic jets and skimmed molecular beams in free-jet zones of silence. *J. Phys. Chem.* **88**(20), 4466–4474 (1984)
- Douglas, D.J., French, J.B.: Collisional focusing effects in radio frequency quadrupoles. *J. Am. Soc. Mass Spectrom.* **3**(4), 398–408 (1992)
- Shaffer, S.A., Tang, K., Anderson, G.A., Prior, D.C., Udseth, H.R., Smith, R.D.: A novel ion funnel for focusing ions at elevated pressure using electrospray ionization mass spectrometry. *Rapid Commun. Mass Spectrom.* **11**(16), 1813–1817 (1997)
- Guevremont, R., Purves, R.W.: Atmospheric pressure ion focusing in a high-field asymmetric waveform ion mobility spectrometer. *Rev. Sci. Instrum.* **70**(2), 1370–1383 (1999)
- Giles, K., Pringle, S.D., Worthington, K.R., Little, D., Wildgoose, J.L., Bateman, R.H.: Applications of a traveling wave-based radio-frequency-only stacked ring ion guide. *Rapid Commun. Mass Spectrom.* **18**(20), 2401–2414 (2004)
- Jugroot, M., Groth, C.P.T., Thomson, B.A., Baranov, V., Collings, B.A., French, J.B.: Coupled gas and ion transport in quadrupole interfaces. *J. Phys. D: Appl. Phys.* **41**(2), 025205 (2008)
- Wilm, M.S., Mann, M.: Electrospray and Taylor-cone theory, Dole's beam of macromolecules at last? *Int. J. Mass Spectrom. Ion Processes* **136**(2), 167–180 (1994)
- El-Faramawy, A., Siu, K.M., Thomson, B.A.: Efficiency of nano-electrospray ionization. *J. Am. Soc. Mass Spectrom.* **16**(10), 1702–1707 (2005)
- Niessen, W.M.A., Tjaden, U.R., van der Greef, J.: Strategies in developing interfaces for coupling liquid chromatography and mass spectrometry. *J. Chromatogr. A* **554**(1/2), 3–26 (1991)
- Niessen, W.M.A.: Advances in instrumentation in liquid chromatography mass spectrometry and related liquid-introduction techniques. *J. Chromatogr. A* **794**, 407–435 (1998)
- Niessen, W.M.A.: Progress in liquid chromatography-mass spectrometry instrumentation and its impact on high-throughput screening. *J. Chromatogr. A* **1000**, 413–436 (2003)
- Manisali, I., Chen, D.D.Y., Schneider, B.B.: Electrospray ionization source geometry for mass spectrometry: past, present, and future. *Trends Anal. Chem.* **25**(3), 243–256 (2006)
- Major, M., Bajic, S., Bristow, A., Ray, A.: A novel source design for the analysis of both polar and non-polar species. Poster presented at the 60th ASMS Conference, Vancouver (2012)
- Aqai, P., Blesa, N.G., Major, H., Pedotti, M., Varani, L., Ferrero, V.E., Nielen, M.W.: Receptor-based high-throughput screening and identification of estrogens in dietary supplements using bio-affinity liquid-chromatography ion mobility mass spectrometry. *Anal. Bioanal. Chem.* **405**(29), 9427–9436 (2013)
- Lubin, A., Geerinx, S., Bajic, S., Cabooter, D., Augustijns, P., Cuyckens, F., Vreeken, R.J.: Enhanced performance for the analysis of prostaglandins and thromboxanes by liquid chromatography-tandem mass spectrometry using a new atmospheric pressure ionization source. *J. Chromatogr. A* **1440**, 260–265 (2016)
- Bajic, S.: U.S. Patent No. 8,809,777. U.S. Patent and Trademark Office, Washington, DC (2014)
- Chubaty, N.D., Wang, T., McEwen, C.N.: More inclusive or selective ionization for mass spectrometry using obstructive sonic spray ionization and voltage polarity switching. *Rapid Commun. Mass Spectrom.* **26**(23), 2763–2769 (2012)
- Coandă, H.: Procédé et dispositif pour faire dévier une veine de fluide pénétrant dans un autre fluide. Brevet d'invention France. no. 792.754 /08.10 (1934)

23. Cîrciu, I., Dinea, S.: Review of applications on Coandă effect. History, theories, new trends. *Rev. Air Force Acad.* **2**, 14 (2010)
24. McGill, R., Tukey, J.W., Larsen, W.A.: Variations of box plots. *Am. Stat.* **32**(1), 12–16 (1978)
25. Krzywinski, M., Altman, N.: Points of significance: visualizing samples with box plots. *Nat. Methods* **11**(2), 119–120 (2014)
26. Kebarle, P.: A brief overview of the present status of the mechanisms involved in electrospray mass spectrometry. *J. Mass Spectrom.* **35**(7), 804–817 (2000)
27. Juraschek, R., Dülcks, T., Karas, M.: Nanoelectrospray—more than just a minimized-flow electrospray ionization source. *J. Am. Soc. Mass Spectrom.* **10**(4), 300–308 (1999)
28. Grimm, R.L., Beauchamp, J.L.: Evaporation and discharge dynamics of highly charged droplets of heptane, octane, and p-xylene generated by electrospray ionization. *Anal. Chem.* **74**(24), 6291–6297 (2002)
29. Akhtar, S.W., Nasr, G.G., Yule, A.J.: Characteristics of water droplet impaction behavior on a polished steel heated surface: Part I. *Atomization Sprays* **17**(8), 659–681 (2007)
30. Dumitrache, A., Frunzulica, F., Ionescu, T.C.: Mathematical modelling and numerical investigations on the Coanda effect. In: Awrejcewicz, J. (ed.) *Nonlinearity, bifurcation and chaos - theory and applications*, InTech (2012). doi:10.5772/50403. Available from: <http://www.intechopen.com/books/nonlinearity-bifurcation-and-chaos-theory-and-applications/mathematical-modelling-and-numerical-investigations-on-the-coanda-effect>
31. Kestin, J., Wood, R.T.: On the stability of two-dimensional stagnation flow. *J. Fluid Mech.* **44**(03), 461–479 (1970)
32. Bajic, S.: PCT Patent application, international publication number WO 2016/027073 A1. (2016)
33. Loeb, L.B.: *Static electrification*. Springer-Verlag OHG, Berlin (1958)
34. Robb, D.B., Covey, T.R., Bruins, A.P.: Atmospheric pressure photoionization: an ionization method for liquid chromatography-mass spectrometry. *Anal. Chem.* **72**(15), 3653–3659 (2000)
35. Katta, V., Rockwood, A.L., Vestal, M.L.: Field limit for ion evaporation from charged thermospray droplets. *Int. J. Mass Spectrom. Ion Processes* **103**(2), 129–148 (1991)
36. Yarin, A.L.: Drop impact dynamics: splashing, spreading, receding, bouncing. *Annu. Rev. Fluid Mech.* **38**, 159–192 (2006)
37. Josserand, C., Thoroddsen, S.T.: Drop impact on a solid surface. *Annu. Rev. Fluid Mech.* **48**, 365–391 (2016)